Radiative Auger spectra of several K and Ca compounds

1996 J. Phys.: Condens. Matter 8 37

(http://iopscience.iop.org/0953-8984/8/1/006)

J. Phys.: Condens. Matter **8** (1996) 37–46. Printed in the UK

Radiative Auger spectra of several K and Ca compounds

Hisashi Hayashi, Noboru Watanabe and Yasuo Udagawa

Research Institute for Scientific Measurements, Tohoku University, Katahira 2-1-1, Sendai, 980-77, Japan

Received 19 September 1995, in final form 14 November 1995

Abstract. K–MM radiative Auger (RA) spectra have been measured for several compounds containing K and Ca. Transition energies are evaluated by the use of various sources: the DV-X_α calculation, term values from optical spectroscopy, and L–MM Auger energies. It is shown that the DV-X_α calculation is very useful in the understanding of RA spectra; calculated transition energies agree well with observed ones as well as those estimated from optical data, giving an unambiguous assignment for the observed spectra. On the other hand, transition energies evaluated from L–MM Auger energies sometimes disagree with others. Possible reasons for the discrepancy are discussed.

1. Introduction

In x-ray fluorescence spectra of the fourth-row elements, weak satellite bands called Kη are observed on the low-energy side of the K$\beta_{1,3}$ main line. These have been interpreted in terms of K–MM radiative Auger (RA) transitions (Åberg 1971). Figure 1 shows a schematic illustration of this transition (b) as well as of the well known Kβ fluorescence (a) and the Auger transition (c). In RA transitions an emission of an x-ray photon and an excitation of an outer-shell electron take place simultaneously when an inner-shell hole is filled with an outer-shell electron. If the final state of an RA transition is a bound state, the emission spectrum is expected to be discrete. On the other hand, if the final state is a continuum, the spectrum should show an asymmetric profile with an edge on the high-energy side, reflecting the density of the final states. RA transitions are of interest because their energies correspond to soft x-rays although they are observed in hard x-ray spectra; thus they appear, like x-ray Raman spectroscopy (Tohji and Udagawa 1989), to provide a possible alternative to soft x-ray absorption spectroscopy for probing bulk instead of surface properties (Kawai *et al* 1994).

K–MM RA spectra have been extensively studied for Ar experimentally (Keski-Rahkonen and Utriainen 1974) as well as theoretically (Kostroun and Baptista 1976). In these studies, two different means have been employed to evaluate RA transition energies. One is based upon optical (VUV-SX) spectroscopy (Moore 1949, Minnhagen 1963), while the other uses energies calculated from the experimental L–MM Auger spectrum (Siegbahn *et al* 1969). RA transition energies evaluated by the two the methods agree quite well with each other and also correspond to the observed ones.

K–MM RA spectra from K to Zn in several compounds have been reported (Utriainen and Åberg 1971, Servomaa and Keski-Rahkonen 1975, Kasrai and Urch 1978, Keski-Rahkonen and Ahopelto 1980, Nigam and Soni 1981, Budnar *et al* 1992, Kawai *et al* 1994). In most of these studies observed bands have been interpreted in terms of L–MM

0953-8984/96/010037+10$19.50

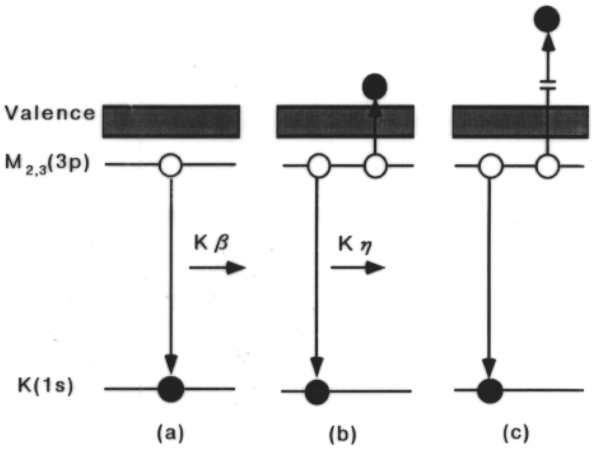

Figure 1. A schematic illustration of (a) a Kβ radiative transition, (b) a K–MM radiative Auger transition, and (c) a non-radiative (Auger) transition.

Auger energies; this is simply because optical data are lacking other than for atoms or ions isoelectronic with Ar.

Doubt may be cast, however, on the soundness of the assignments based solely on L–MM Auger energies. In these studies only transitions to continua are taken into consideration in spite of the fact that rates of transition to discrete states are estimated to amount to a quarter of the total rates in Ar (Kostroun and Baptista 1976). In addition, L–MM Auger energies in compounds may be subject to various solid-state effects. Indeed, a study on RA transitions of K^+ ions using optical data (Utriainen and Åberg 1971) gave an assignment different from that based on L–MM Auger energies (Nigam and Soni 1981). Hence some other approaches are needed to render the understanding of these satellites assured.

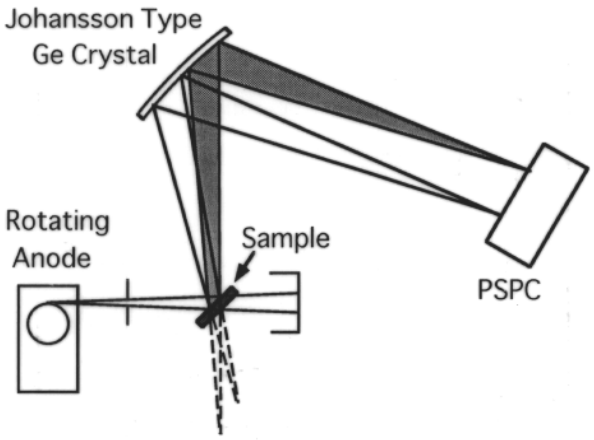

Figure 2. The experimental system.

In this study RA spectra of several K and Ca compounds were measured and assignments of prominent peaks are attempted with the aid of DV-X_α calculations. The DV-X_α method is widely used to calculate various properties of matter (Adachi *et al* 1978) and has been

employed in several studies concerning transitions involving K electrons such as XANES (Nakamatsu *et al* 1991) and x-ray fluorescence investigations (Kawai *et al* 1986). It has, however, not been applied with the aim of explaining RA spectra in which transitions of two electrons are concerned.

The elements studied here were chosen because their ions are isoelectronic with Ar and hence a comparison with transition energies calculated from optical data (hereafter called optical RA energies) as well as those from L–MM Auger energies (L–MM Auger RA energies) is possible. Several compounds were studied with the aim of observing possible chemical effects on RA transitions.

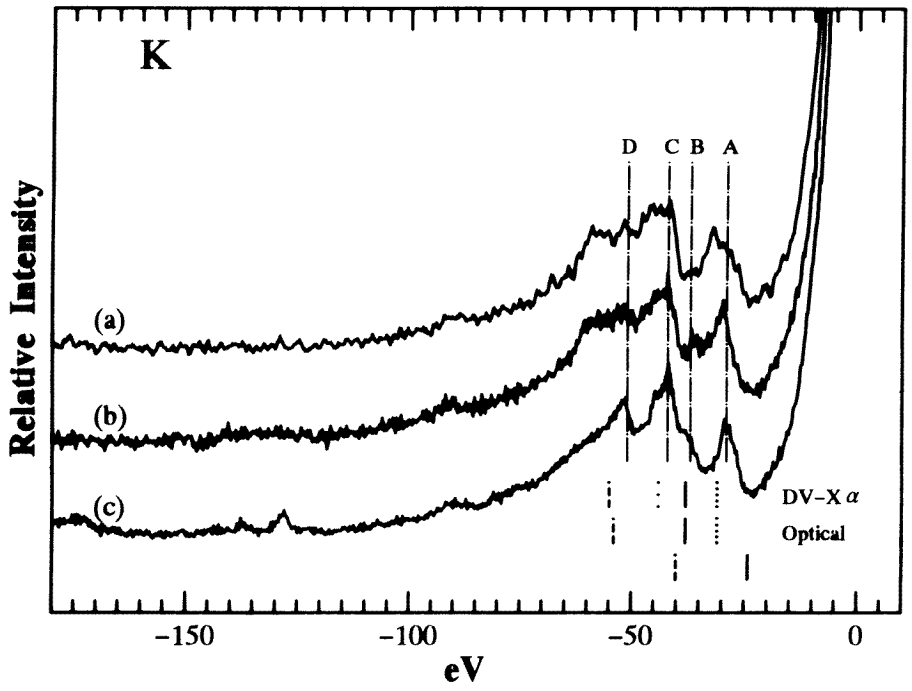

Figure 3. K–MM RA spectra of (a) KCl, (b) K_2SO_4, and (c) KF. The lines ·····, ——, ... and - - - - indicate the average transition energies of K–$M_{2,3}M_{2,3}$ ($1s^{-1} \rightarrow 3p^{-2}4p$), K–$M_{2,3}M_{2,3}$ ($1s^{-1} \rightarrow 3p^{-2}$), K–$M_1M_{2,3}$ ($1s^{-1} \rightarrow 3s^{-1}3p^{-1}4s$), and K–$M_1M_{2,3}$ ($1s^{-1} \rightarrow 3s^{-1}3p^{-1}$) RA transitions, respectively. A weak peak at −127 eV in the KF spectrum is due to a diffraction because it moves with changes in the detection angle.

2. Experimental procedure

X-ray spectra were measured using a spectrometer shown schematically in figure 2. A Ge(220) Johansson-type crystal was employed as the analysing crystal. The crystal has a radius of curvature of 320 mm and was mounted at 150 mm from the sample. A position-sensitive proportional counter (PSPC) coupled with a multichannel analyser was employed as an x-ray detector. The effective length and the space resolution of the detector are 100 and 0.2 mm, respectively. The energy calibration was performed by the use of the K $K\beta_{1,3}$, Ca $K\beta_{1,3}$, and Ba $L\ell$ lines. The resolution was estimated to be about 3 eV at 4 keV from the FWHM of the Ca $K\beta_{1,3}$ line.

Table 1. K–MM RA transition energies relative to K$\beta_{1,3}$ lines (eV).

RA transition		Auger†	Optical‡	DV-Xα Multiplet§	DV-Xα Average‖	Experimental¶
Ar						
K–M$_{2,3}$M$_{2,3}$						
($1s^{-1} \rightarrow 3p^{-2}4p$)						
	^{3}P	—	−19.9[a]	−19.3		−22(A)[b]
	^{1}D	—	−21.4[a]	−21.2	−20.7	
	^{1}S	—	−23.8[a]	−24.9		−25(B)[b]
($1s^{-1} \rightarrow 3p^{-2}$)						
	^{3}P	−27.6[a]	−27.6[c]	−26.9		
	^{1}D	−29.4[a]	−29.4[d]	−28.8	−27.9	
	^{1}S	−31.6[a]	−31.7[d]	−32.6		
						−35(C)[b]
K–M$_1$M$_{2,3}$						
($1s^{-1} \rightarrow 3s^{-1}3p^{-1}4s$)						
	^{3}P	—	−30.1[a]	−29.1	−30.8	
	^{1}P	—	−33.3[a]	−35.9		
($1s^{-1} \rightarrow 3s^{-1}3p^{-1}$)						
	^{3}P	−41.5[a,e]	−41.7[d]	−39.6	−41.3	−43(D)[b]
	^{1}P	−45.3[a,e]	−45.4[c]	−46.4		−47(E)[b]
K						
K–M$_{2,3}$M$_{2,3}$						
($1s^{-1} \rightarrow 3p^{-2}4p$)						
	^{3}P	—	−30[f]	−30		
	^{1}D	—	—	−32	−31	−30(A)
	^{1}S	—	—	−35		
($1s^{-1} \rightarrow 3p^{-2}$)						
	^{3}P	−23.2[g]	−37[f]	−37		
	^{1}D	−25.3[g]	−39[h]	−39	−38	−37(B)
	^{1}S	−26.9[g]	−42[h]	−42		
K–M$_1$M$_{2,3}$						
($1s^{-1} \rightarrow 3s^{-1}3p^{-1}4s$)						
	^{3}P	—	—	−43	−44	−42(C)
	^{1}P	—	—	−50		
($1s^{-1} \rightarrow 3s^{-1}3p^{-1}$)						
	^{3}P	−38.1[e,g]	−54[f]	−53	−55	−51(D)
	^{1}P	−46.0[e,g]	−59[h]	−60		
Ca						
K–M$_{2,3}$M$_{2,3}$						
($1s^{-1} \rightarrow 3p^{-2}4p$)						
	^{3}P	—	−41[i]	−41		
	^{1}D	—	—	−43	−42	−45(A)
	^{1}S	—	—	−47		
($1s^{-1} \rightarrow 3p^{-2}$)						
	^{3}P	−31.2[g,j]	−46[i]	−46		
	^{1}D	−33.4[g,j]	−48[i]	−48	−47	−50(B)
	^{1}S	−35.3[g,j]	−51[i]	−52		
K–M$_1$M$_{2,3}$						
($1s^{-1} \rightarrow 3s^{-1}3p^{-1}4s$)						
	^{3}P	—	—	−55	−57	−57(C)
	^{1}P	—	—	−62		
($1s^{-1} \rightarrow 3s^{-1}3p^{-1}$)						
	^{3}P	−48.0[e,g,j]	−65[i]	−64	−66	−72(D)
	^{1}P	−56.7[e,g,j]	−70[i]	−71		

Table 1. (Continued)

† L–MM Auger RA energies.
‡ Optical RA energies.
§ Multiplet DV-X_α RA energies.
‖ Average DV-X_α RA energies.
¶ Observed peak energies. For A–D of K and Ca, see figures 3 and 4.
(a) Kostroun and Baptista (1976).
(b) Estimated values from the spectrum measured by Keski-Rahkonen and Utriainen (1974). A–E are the symbols employed in their spectrum.
(c) Optical RA energies calculated from Moore's (1949) data.
(d) Optical RA energies calculated from Minnhagen's (1963) data.
(e) Nigam and Soni (1981).
(f) Utriainen and Åberg (1971).
(g) L–MM Auger RA energies calculated from Larkins's (1977) data.
(h) Optical RA energies calculated from Moore's (1949) data and the KF Madelung potential.
(i) Optical RA energies calculated from Moore's (1949) data and the CaO Madelung potential.
(j) Budnar *et al* (1992).

All the compounds were obtained commercially. No trace of impurity fluorescence was detected in the energy region studied. The samples were excited by a direct beam from an x-ray generator (Rigaku, RU-7A) with a Mo target. It was operated at 420 mA and 11 kV to avoid any possible contamination of W impurity lines. Accumulated signals for each spectrum were in the range of 2000 (KCl) to 12 000 (Ca metal) counts at prominent K–MM RA satellite peaks.

3. Results

3.1. Observed RA spectra

Figures 3 and 4 show K–MM RA spectra of several K and Ca compounds. The abscissae give the energies measured from the respective $K\beta_{1,3}$ main lines. K–MM RA spectra of KF and KCl have already been reported (Utriainen and Åberg 1971), and they are almost identical with the ones shown here. Among all the K compounds studied, KF shows the most detailed structure. Hence the energies of prominent peaks of KF spectra indicated in figure 3, trace(c), are given in the sixth column of table 1. In the case where the final state is a continuum, edge energies must be employed to make a comparison with calculated values. However, peak energies are given in the table regardless of the nature of the transitions, since the difference between an edge and the associated peak is less than a few electron volts.

The RA spectrum of Ca has so far been reported (Budnar *et al* 1992) only for the metal. RA spectra of Ca, CaO, and CaF_2 are shown in figure 4. Of these, that for CaF_2 shows the most distinct structure, and in the sixth column of table 1 we give the energies of the peaks of CaF_2 indicated in figure 4, trace (c).

In table 1 the L–MM Auger RA and the optical RA energies estimated from various references are also shown. The optical RA energies for Ca^{2+} are calculated here by the use of the energy levels reported for free ions by Moore (1949). The crystal-field effect is taken into account by subtracting the Madelung energy as was done by Utriainen and Åberg (1971).

3.2. Evaluation of RA transition energies in terms of the DV-X_α calculation

RA transition energies of the Ar atom and K^+ and Ca^{2+} cations were evaluated from the DV-X_α calculation as follows. First, transition energies of four RA transitions shown in the first column of table 1 were calculated by means of Slater's (1979) transition state method. Only these four transitions are allowed from the selection rule proposed by Bloch (1935) and Åberg (1971). In the calculations, 1s–4p numerical atomic orbitals were employed as a basis set for the elements studied here. The exchange scaling parameter, α, was fixed at 0.7. Madelung potentials of KF and CaO were employed to introduce a crystal-field effect. The calculated energies are shown in the fifth column of table 1, and also indicated in figures 3 and 4. These transition energies must be regarded as being the averages of multiplets, because *L–S* coupling was not taken into consideration. For a visual comparison the average transition energies estimated from optical as well as L–MM Auger transitions are marked in figures 3 and 4.

Next, multiple splitting was corrected using Coulomb-type and exchange-type Slater integrals, F^2(3p, 3p) and G^1(3s, 3p) (Slater 1960). The Slater integrals used here were evaluated from the following multiplet energies, $E(3p^2{:}^3P)$, $E(3p^2{:}^1D)$, $E(3s3p{:}^3P)$, and $E(3s3p{:}^1P)$, which were calculated by the DV-X_α method according to Ziegler *et al* (1977). The integral values are listed in table 2 together with those derived from relativistic Hartree–Fock calculations (Larkins 1977) in order to show the accuracy of the DV-X_α calculations. The RA transition energies thus calculated, hereafter called multiplet DV-X_α RA energies, are listed in the fourth column of table 1. In order to make a precise comparison, the L–MM Auger RA energies are also tabulated together with the optical RA energies in the second and third columns of table 1.

Table 2. Calculated Slater integrals in eV.

	DV-$X_\alpha^{(a)}$	HF[(b)]
Ar		
F^2(3p, 3p)	7.8	7.7
G^1(3s, 3p)	10.3	10.8
K		
F^2(3p, 3p)	8.4	8.5
G^1(3s, 3p)	11.5	11.9
Ca		
F^2(3p, 3p)	9.0	9.3
G^1(3s, 3p)	12.4	13.0

[(a)] The Slater integrals calculated by applying the approach of Ziegler *et al* (1977).
[(b)] The Slater integrals derived from relativistic Hartree–Fock calculations (Larkins 1977).

No attempt was made to calculate transition intensities because of the complexity of the matrix elements which govern RA transitions (Kostroun and Baptista 1976).

4. Discussion

4.1. The DV-X_α calculation for Ar

Both the L–MM Auger and the optical RA energies of Ar, being free from possible deviations originating from solid-state effects, should coincide within experimental error.

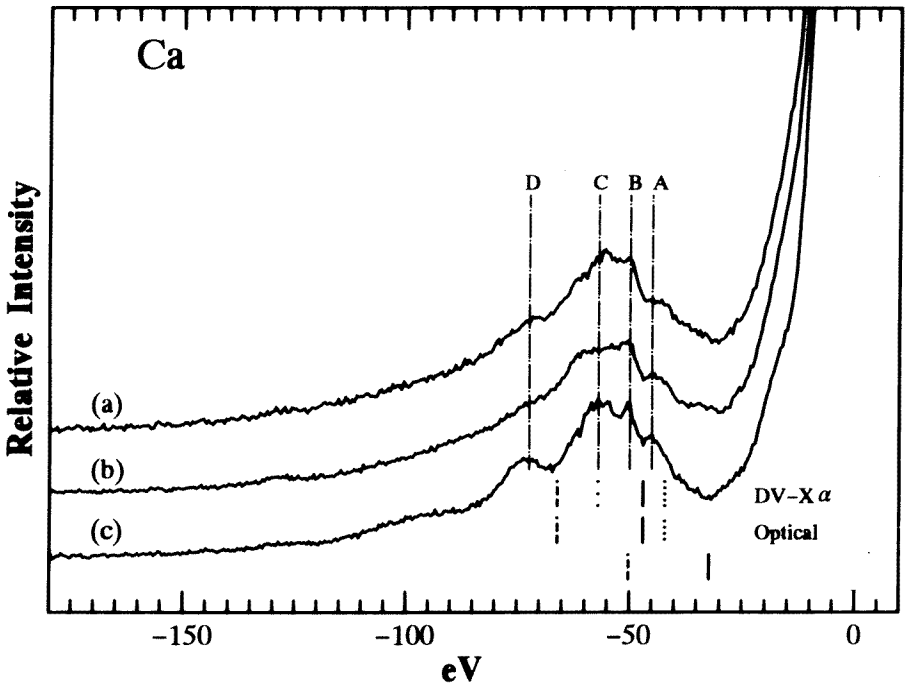

Figure 4. K–MM RA spectra of (a) Ca metal, (b) CaO, and (c) CaF_2. The lines ·····, ——, ... and - - - - indicate the average transition energies of K–$M_{2,3}M_{2,3}$ ($1s^{-1} \rightarrow 3p^{-2}4p$), K–$M_{2,3}M_{2,3}$ ($1s^{-1} \rightarrow 3p^{-2}$), K–$M_1M_{2,3}$ ($1s^{-1} \rightarrow 3s^{-1}3p^{-1}4s$), and K–$M_1M_{2,3}$ ($1s^{-1} \rightarrow 3s^{-1}3p^{-1}$) RA transitions, respectively.

Indeed, as is observable from table 1, they agree quite well with each other where both sets of data are available. Although multiplet splittings are not fully resolved, experimentally observed RA transition energies also correspond to them. Thus the assignments in the table are believed to be correct and accordingly the DV-X_α RA energy calculations for Ar furnish us with an excellent opportunity to check the accuracy of the method.

A comparison of the multiplet DV-X_α RA energies with the L–MM Auger RA as well as the optical RA energies in table 1 proves that the DV-X_α RA energies reproduce the transition energies within 2 eV. The average DV-X_α RA energies also correspond within a few eV to the observed energies. Since no adjustable parameter is involved in the calculation, a similar accuracy is expected for other elements as well.

4.2. K–MM RA spectra of K and Ca ions

Although the assignments for Ar have been firmly established, two different sets of assignments have been proposed for K–MM RA spectra of KF and KCl as described in the introduction. As shown in table 1, one, based on the L–MM Auger energies, attributes the observed spectra to transitions to two continua, while the other attributes them to transitions to both continuum and bound states from the optical RA energies.

The multiplet DV-X_α RA energies for KF shown in table 1 coincide well with the optical RA energies but do not agree with the L–MM Auger RA energies, thus supporting the assignment given by Utriainen and Åberg (1971). Observed spectra can be interpreted

on the basis of the average DV-X_α RA energies in the following manner. The first peak A, which is symmetric and hence must be related to a transition to a bound state, is assigned to the $1s^{-1} \rightarrow 3p^{-2}$ 4p transition. The next features, B and C, are assigned to the transitions to the $3p^{-2}$ continuum state and to the discrete $3s^{-1}3p^{-1}4s$ state, respectively. The observed band shape is in accordance with the assignment. The feature D, which has a sharp edge followed by a gradual decay, is assigned to the transition to the continuous $3s^{-1}3p^{-1}$ state on the basis of the energy as well as on the basis of the band shape. The order of the transitions proposed here for K^+ is the same as that for Ar.

RA spectra of other K compounds are somewhat more diffuse and thus are not amenable to detailed discussion based on band shapes and energies. They can, however, be interpreted in a similar fashion because the spectra resemble that of KF as is shown in figure 3, and the DV-X_α calculations give similar results.

Budnar *et al* (1992) observed two edges in the RA spectrum of Ca metal excited with high-energy protons and assigned them to transitions to two continuum states, namely $3p^{-2}$ and $3s^{-1}3p^{-1}$, on the basis of L–MM Auger energies. As the RA spectrum of CaF_2 obtained here is much sharper than that of Ca metal, it is possible to distinguish four features as indicated in figure 4. The number corresponds to that of the expected allowed transitions, but the features are not distinct enough to be assigned with the aid of band shapes. In this case too, however, the multiplet DV-X_α RA energies agree quite well with those calculated from the optical data (Moore 1949). The average DV-X_α RA energies correspond also to the energies of the observed features. Thus the assignments shown in table 1 are proposed.

It should be emphasized here that, contrary to what is assumed in making the assignments in most previous studies on K–MM RA spectra, transitions to discrete states cannot be neglected in spite of the fact that observed bands are often broad.

4.3. The chemical effect on the K–MM RA band width

No appreciable chemical shift is observed in figures 3 and 4—or, if it does exist, it is hidden by the broadness of the bands. On the other hand, spectral width varies from element to element, and even for the same element it depends on the chemical environment. From the data presented here, a distinct tendency can be noted for both K and Ca: more ionicity means sharper structure.

The reason for this can be understood qualitatively on the basis of the observation above that not only transitions to continuum states but also those to discrete final states contribute to RA spectra. In solids a discrete state of an atom or an ion makes a band which makes a final state of RA transitions. The band width depends on the interatomic interactions in the compound and broadens with increasing covalency. Thus reduced ionicity results in broader RA spectra.

5. Comparisons of the bases for the assignments of RA transitions

In the previous section it has been established that the multiplet DV-X_α RA energies coincide very well with the optical RA energies. This is not accidental, from the viewpoint that both assume the same crystal-field effect. In the calculations of the optical RA energies, transition energies are estimated first from the energy levels observed in the gas-phase absorption spectra. Madelung energies are then subtracted as the crystal-field effect. Energy levels calculated by the DV-X_α method are also for free atoms, and the crystal-field effect is again taken into consideration as the Madelung potential. Since the DV-X_α calculation gives accurate energy levels for free Ar, transition energies for the atoms in the crystal must

also coincide. Although optical data are not always available for calculating RA transition energies, the DV-X_α calculations can conveniently be carried out for any element. Since the accuracy of the DV-X_α calculation as regards achieving an understanding of K–MM RA transitions has been proved in the present study, it could be applied for various other elements.

On the other hand, at present we cannot specify why estimations from observed L–MM Auger spectra sometimes fail to predict correct RA transition energies in solids. One obvious reason is that only transitions to continua can be evaluated from L–MM Auger spectra, although those to discrete states also contribute to RA spectra. Several other possibilities, however, can be conceived of. Since an emission of Auger electrons from solids is surface sensitive but the RA process is not, differences in electronic states between the surface and the bulk may be responsible. Chemical shifts among compounds are also likely to contribute to the observed discrepancy; for example, Väyrynen *et al* (1990) reported that the chemical shift of L–MM Auger spectra amounts to as much as 10 eV—or more—for metallic Ca and CaO. In a study on RA spectra of several iron compounds, Kasrai and Urch (1978) observed that K–MM RA transition energies of metallic iron agree remarkably well with L–MM Auger RA energies of iron metal, but those of some other iron compounds do not, indicating that chemical shifts can account for the discrepancies. L–MM Auger transition energies of other iron compounds were not available in their study. Few studies of L–MM Auger transitions have been made for insulators because of possible space-charge effects, which may account for apparent chemical shifts.

6. Conclusion

In this study the nature of the K–MM RA bands of K^+ and Ca^{2+} has been demonstrated to have the same origin as that for the isoelectronic atom, Ar. The DV-X_α calculation is found to be very suitable for use in analysing K–MM RA transitions in which two electrons are involved. It is thus expected to be also applicable to other multiple-electron processes such as shake-up or shake-off of satellites in XPS.

Acknowledgments

We thank Dr J Kawai and Dr H Nakamatsu of Kyoto University for their support in the DV-X_α calculation and helpful discussions. We are indebted to the staff of the machine shop at the Research Institute for Scientific Measurements for the construction of the x-ray spectrometer.

References

Åberg T 1971 *Phys. Rev.* A **4** 1735–40
Adachi H, Tsukada M and Satoko C 1978 *J. Phys. Soc. Japan* **45** 875–83
Bloch F 1935 *Phys. Rev.* **48** 187–92
Budnar M, Mühleisen A, Hribar M, Janžekovič H, Ravnikar M, Šmit Ž and Žitnik M 1992 *Nucl. Instrum. Methods* B **63** 377–83
Kasrai M and Urch D S 1978 *Chem. Phys. Lett.* **53** 539–41
Kawai J, Nakajima T, Inoue T, Adachi H, Yamaguchi M, Maeda K and Yabuki S 1994 *Analyst* **119** 601–3
Kawai J, Satoko C, Fujisawa K and Gohshi Y 1986 *Phys. Rev. Lett.* **57** 988–91
Keski-Rahkonen O and Ahopelto J 1980 *J. Phys. C: Solid State Phys.* **13** 471–82
Keski-Rahkonen O and Utriainen J 1974 *J. Phys. B: At. Mol. Phys.* **7** 55–58
Kostroun V O and Baptista G B 1976 *Phys. Rev.* A **14** 363–79

Larkins F P 1977 *At. Data Nucl. Data Tables* **20** 311–87
Minnhagen L 1963 *Ark. Fys.* **25** 203–85
Moore C E 1949 *Atomic Energy Levels (NBS Circular No 467)* vol 1 (Washington, DC: US Government Printing Office)
Nakamatsu H, Mukoyama T and Adachi H 1991 *J. Chem. Phys.* **95** 3167–74
Nigam A N and Soni S N 1981 *J. Phys. C: Solid State Phys.* **14** 3289–95
Servomaa A and Keski-Rahkonen O 1975 *J. Phys. C: Solid State Phys.* **8** 4124–30
Siegbahn K *et al* 1969 *ESCA Applied to Free Molecules* (Amsterdam: North-Holland)
Slater J C 1960 *Quantum Theory of Atomic Structures* vol 1 (New York: McGraw-Hill)
——1979 *The Calculation of Molecular Orbitals* (Chichester: Wiley)
Tohji K and Udagawa Y 1989 *Phys. Rev.* B **39** 7590–4
Utriainen J and Åberg T 1971 *J. Phys. C: Solid State Phys.* **4** 1105–7
Väyrynen I J, Leiro J A and Heinonen M H 1990 *J. Electron Spectrosc. Relat. Phenom.* **51** 555–64
Ziegler T, Rauk A and Baerends E J 1977 *Theor. Chim. Acta* **43** 261–71